HHS Public Access

Author manuscript

J Bio Tribocorros. Author manuscript; available in PMC 2022 June 01.

Published in final edited form as:

J Bio Tribocorros. 2021 June ; 7(2): . doi:10.1007/s40735-021-00486-8.

Diabetes as a Risk Factor for Orthopedic Implant Surface Performance: A Retrieval and *In Vitro* Study

Alexandra Arteaga, MS,
Department of Biomedical Engineering, University of Texas at Dallas, Richardson, TX, USA

Jiayi Qu,
Department of Interdisciplinary Studies, University of Texas at Dallas, Richardson, TX, USA

Sara Haynes, MD,
Department of Orthopaedic Surgery, John Peter Smith Hospital, Ft. Worth, TX, USA

Brian G. Webb, MD,
Department of Orthopaedic Surgery, John Peter Smith Hospital, Ft. Worth, TX, USA

Javier LaFontaine, MD,
Department of Plastic Surgery, University of Texas Southwestern Medical Center, Dallas, TX, USA

Danieli C. Rodrigues, PhD
Department of Biomedical Engineering, University of Texas at Dallas, Richardson, TX, USA

Abstract

Orthopedic devices are often associated with increased risk for diabetic patients due to impaired wound healing capabilities. Adverse biological responses for immunocompromised patients at the implant-tissue interface can lead to significant bone resorption that may increase failure rates. The goal of this study was to characterize the surface of implants removed from diabetic patients to

Alexandra.Arteaga@utdallas.edu.

Authors' contributions: Alexandra Arteaga and Dr. Danieli Rodrigues conceived the ideas for this manuscript. Alexandra Arteaga and Jiayi Qu conducted all surface analyses for implant retrievals and in vitro studies. Dr. Sara Haynes and Dr. Brian Webb obtained/collected the orthopedic implants, removed all identifiers, and pooled specific clinical data related to the implants. Dr. Javier LaFontaine assisted in manuscript writing and editing. Dr. Danieli Rodrigues supervised the project and also assisted in manuscript writing and editing.

Conflicts of interest/Competing interests: All authors certify that they have no affiliations with or involvement in any organization or entity with any financial interest or non-financial interest in the subject matter or materials discussed in this manuscript.

Declarations

Ethics approval: All authors received Institutional Review Board approval (IRB 19–85) prior to any research conducted in this manuscript. All retrieved implants were deidentified, and all clinical information collected associated with that implant were linked to the letter/number and not to the name of the patient or any other identifiable personal health information. Only the hospital had access to patient information and identifiers. Researchers did not have access to personal identifiers.

Consent to participate: Not applicable.

Consent for publication: All authors consent to the publication of the current manuscript, should the article be accepted by Editor-in-chief upon completion.

Availability of data and material: Data available within the article.

Code availability: Not applicable.

determine underlying mechanisms of diabetes-induced impaired osseointegration. Thirty-nine retrieved titanium and stainless-steel orthopedic devices were obtained from diabetic and non-diabetic patients, and compared to non-implanted controls. Optical Microscopy, Scanning Electron Microscopy, Energy Dispersive X-ray Spectroscopy, and X-ray Photoelectron Spectroscopy revealed changes in morphology, chemical composition, oxidation state, and oxide thickness of the retrieval specimens, respectively. Additionally, titanium disks were immersed for 28 days in simulated *in vitro* diabetic conditions followed by Inductively Coupled Plasma-Optical Emission Spectroscopy to quantify metal dissolution. Electrochemical testing was performed on specimens from retrievals and *in vitro* study. Aside from biological deposits, retrievals demonstrated surface discoloration, pit-like formations and oxide thinning when compared to non-implanted controls, suggesting exposure to unfavorable acidic conditions. Cyclic load bearing areas on fracture-fixation screws and plates depicted cracking and delamination. The corrosion behavior was not significantly different between diabetic and non-diabetic conditions of immersed disks or implant type. However, simulated diabetic conditions elevated aluminum release. This elucidates orthopedic implant failures that potentially arise from diabetic environments at the implant-tissue interface. Design of new implant surfaces should consider specific strategies to induce constructive healing responses in immunocompromised patients while also mitigating corrosion in acidic diabetic environments.

Keywords

Diabetes; Orthopedic Implants; Retrieval; Titanium Alloy; Stainless Steel

1. Introduction

While orthopedic device implantation is widely considered a relatively safe and predictable procedure, patients still experience failure rates that range between 4.9% and 14.4% after an average of 6.5 years post-implantation due to varying underlying pathologies [1]. Orthopedic implants are considered higher risk for patients that have compromised wound healing capabilities from disorders like diabetes mellitus, which can consequently lead to implant failure [2]. In 2018, 34.2 million Americans were reported to have diabetes, which translates to 10.5% of the population with an estimated increase of 1.5 million per year [3]. Complications arising from poorly controlled diabetes have been shown to negatively impact bone metabolism, growth factor expression, cartilage formation, and neurovascularization [4]. Despite these findings, there is limited evidence from retrieval studies addressing the difference seen in failure rates between diabetic and non-diabetic patients [4]. Common causes of early implant failure include corrosion of the surface, micromotion, infection of the surrounding tissues, and surgical error. Clinical consequences of implant failure include nonunion, malunion of fractures, and implant loosening. Through analysis of implant surface morphological features, the extent of the biological issues can be further identified and quantified [5].

Surface level diffusion of metal ions through an intact oxide layer typically occurs at minute amounts, but a compromised oxide layer resulting from damage due to corrosion, pitting, mechanical scratches, and stress may result in large amounts of metal ions and debris

released causing severe inflammatory responses [6]. Surface characteristics are recognized to play a crucial role in modulating tissue response to implants, including the extent of the bone-implant osteointegration, which is vital to retention of the implant. In the absence of applied mechanical loading, studies have shown that mature osteoclasts alone are able to directly corrode titanium, aluminum and stainless steel, which resulted in increased metal ion release that induce the secretion of pro-inflammatory cytokines [7]. Sustained inflammation leads to both deterioration of healthy bone at the local level and systemic buildup of metal ions as they are transported via protein transport in the bloodstream and lymph fluid [8]. Biological responses to products released from these degradation processes can lead to decreased osteoblast activity and significant bone loss [8].

Previous retrieval studies have shown that wear and stress-corrosion fatigue are the most common causes of orthopedic implant failures [9]. Corrosion may lead to total failure of the implant, third body wear from particles trapped between articulating surfaces [10], osteolysis, and local granulomatous reactions. Topographic analyses of retrieved implants from total hip and knee implants demonstrated surface fretting corrosion and wear through abrasion and deformation of load bearing surfaces [9]. Modularity between implant components greatly increases the amount of debris produced from both fretting and crevice corrosion, leading to an increased focus on tribocorrosion [10]. Repassivation of the damaged surface results in a peri-implant buildup of H^+ and Cl^- ions that lower the pH within the crevice fluidic environment, sustaining corrosion processes [11]. Additional hip implant retrieval studies have shown that wear debris can contribute to osteolysis and aseptic loosening at screw holes through the formation of granulomatous tissue at the bone-implant interface [9]. Metal corrosion products have been shown to migrate along prostheses components and accumulate in the surrounding tissue, which poses significant implications for larger and more pervasive implants [8].

While many studies have elucidated these mechanisms as the most common with orthopedic implants, very few studies have fully explored the role or contribution of a diabetic environment in triggering or sustaining these mechanisms. Previous literature has found that diabetic patients were statistically more likely to require surgical interventions ($p<0.001$) for either irrigation and debridement or amputation within 136 days compared to their non-diabetic counterparts [12]. Diabetes mellitus is a metabolic disease characterized by hyperglycemia along with a chronic inflammatory response that affects fibrogenesis, collagen synthesis, tensile strength, angiogenesis, and the production of cytokines. A combination of these factors and the microvascular disease associated with diabetics lead to delayed or incomplete wound healing [6, 13]. Following surgery, physiological stress alters glucose homeostasis and influences the early healing response, inducing chronic inflammation [14]. Uncontrolled diabetes can lead to a reduced response of cytotoxic and helper T cells, issues with humoral B-cells, and neutrophil dysfunction, limiting healing abilities [15]. Diabetic patients undergoing total joint arthroplasty also exhibit 10% higher infection rates than non-diabetic patients which contributes to poor osseointegration at the implant-tissue interface [16]. Diabetics usually have a decrease in osteoprogenitor cell recruitment activity and suppressed expression of osteogenesis related genes [17]. The diabetic environment has also been found to increase bone resorption, with increased reactive oxygen species production and activation of RANKL protein osteoclast activation

[18]. Much of the literature concerning corrosion of implants in diabetic environments focuses on dental implants, with few having been conducted specifically on orthopedic implants. However, studies on commercial Ti orthopedic implants have found that exposure to lower pH values and higher dextrose concentrations resulted in increased corrosion rates compared to implants immersed in Ringer's solution *in vitro* [19]. Other studies have found that in acidic conditions, such as seen with diabetic ketoacidosis, there is decreased corrosion resistance, indicating that repassivation was hindered by the deviation of pH from the physiological norm [5]. Further research demonstrated that in the presence of hydrogen peroxide (H_2O_2) and albumin, the electrochemical potential dependent passivation of commercially pure Ti alloy was disturbed and a higher current density was seen in titanium alloys [20]. Additional work showed that the rate of Ti alloy corrosion was increased when H_2O_2 and albumin were examined in conjunction with inflammatory products such as reactive oxygen species *in vitro* [21]. This holds relevance to the study of orthopedics in relation to Type 2 Diabetes Mellitus (T2DM) patients, where oxidative stress resulted in H_2O_2 concentrations four times that of non-diabetics [22].

Given the lack of clarity in regard to the impact of diabetes on the surface performance of orthopedic implants and to address the question of why implants fail at a higher rate for diabetic patients, the goal of this study is to investigate the surface characteristics, morphological features, and corrosion behavior of orthopedic implants retrieved in various early and late stages of failure of diabetics. Furthermore, characterization of explanted surfaces and analysis of metal ion elution after immersion of metallic disks under simulated diabetic conditions can help inform the design of future surface modification procedures.

2. Materials and Methods

2.1 Implant Specimens

After Institutional Review Board approval (IRB 19–85), thirty-nine explanted metallic (titanium alloy (Ti6Al4V) and stainless-steel (SS)) orthopedic implants from internal fixation of fractures (ankles, wrists, and long bones) were obtained from the Department of Orthopaedic Surgery at John Peter Smith Hospital (Ft. Worth, TX). The number of implants used for this study was determined solely by the amount of previously retrieved implants that were available at the John Peter Smith Hospital. Table 1 summarizes the received implants. A preliminary visual inspection and classification of the implants was initially performed to identify the severity of damage present (scratches, discoloration, cracking, metallic debris/imperfections, and biological deposits on the surface). Implants were then separated into groups of screws, plates, and intramedullary rods for further analysis (Table 1).

Sample Preparation—Following de-identification, implants were each ultrasonicated three times at 15-minute time intervals each in acetone, then in deionized (DI) water, and finally in ethanol to remove biological and non-biological debris. Implant specimens were then cut into three rectangular-shaped sections with 5–15 mm^2 of bone contacting surface area using an automated saw (Pace Technologies). Samples underwent further

ultrasonication in each of the three solvents listed above to remove potential debris produced during the cutting process.

2.2 *In Vitro* Testing under simulated Diabetic Conditions

Sample Preparation—Metallic disks of titanium alloy (Ti6AL4V) were cut and polished to be a clinically relevant surface (3 mm ø x 2 mm, McMaster Carr). The number of samples was selected in triplicates, taking into consideration the different experimental immersion fluids (DMEM, artificial saliva, and PBS) in combination with either high or low solute concentrations (glucose, urea, beta-hydroxybutyrate). Non-immersed samples and both positive and negative controls were also accounted for in the total number of samples to accurately assess the effects of solutes that could be present in the biological environment. Although the surface of titanium is considered to be chemically stable, the biological capability of titanium to attract proteins and osteogenic cells can change over time, especially in a wet environment. The number of days that the samples were immersed for was selected based on the endochondral ossification process, which should show a hard callous formation 28 days after injury. During this time, any release of ions could significantly affect the early healing process. Previous studies have also shown to analyze metallic samples after 28-day immersion periods [23,24]. Samples were polished until mirror-like surface finish using an automated polisher (NANO 1000T and FEMTO 1100, Pace Technologies) to simulate the current industry standard for removing lines following the casting and grinding process for the majority of orthopedic implants [23]. Disks were then ultrasonicated for 15-minute time intervals in acetone, DI water, and ethanol to remove all potential debris from polishing as performed with received retrieved implant specimens.

Immersion Solution Preparation—To assess surface responses to fluidic environments, metal disks were subjected to immersion in different fluids (glucose-free Dulbecco's Modified Eagle Medium (DMEM, Gibco, Carlsbad, CA), Fusayama/Meyer Artificial saliva (Pickering Laboratories, Mountain View, CA), and phosphate buffered saline (PBS) as a control) in 24-well plates which were sealed to prevent evaporation. Solutes including glucose, urea, and beta-hydroxybutyrate (Beta-OH) were used in diabetic and non-diabetic concentrations based on previous literature (Table 2) to assess potential for accelerated metallic corrosion. Table 2 shows the concentrations of each solute within the immersion media. Concentrations of each solute within DMEM correlate to the concentrations found in blood [24, 25]. Concentrations of each solute in PBS were chosen based on the highest values used between DMEM and artificial saliva [26]. Although saliva is not specifically relevant to the environment in which orthopedic implants are exposed to, this medium was included in the study to represent another physiological scenario where titanium can be exposed in acidic conditions (e.g. in the case of dental implant components). Artificial saliva represents the naturally more acid environment found in the oral cavity; thus, it could prove another interesting medium to further compare surface changes between diabetics and non-diabetics populations. Citric acid (30% w/w in DI water) was used as a positive control. The following treatment groups were studied: citric acid (CA), immersion control (IC), glucose in high (HG) and low (LG) concentrations, urea in high (HU) and low (LU) concentrations, beta-hydroxybutyrate in high (HB) and low (LB) concentrations, and the untreated non-immersed (NI) control. "High" treatments represented simulated diabetic environments, and

"Low" treatments represented simulated non-diabetic environments. Additionally, pH measurements were taken before and after 28-day immersion at 37 °C to evaluate the fluid response to the metal disks.

***In vitro* Analysis of Metal Dissolution in Immersion Fluids—**Inductively Coupled Plasma-Optical Emission Spectroscopy (ICP-OES) (Perkin Elmer Optima 5300 DV, Waltham, MA) was used to quantify the amount of metal dissolution present in each immersion fluid after metal disks were immersed for 28 days. The carrier gas tube and a torch tube made of quartz were connected to a radio-frequency (RF) generator. Argon was introduced to the torch and RF applied to create a magnetic field, initiating production of ions and electrons. As the resultant current flow heated the gas, the introduced sample in the nebulizer was converted to aerosol and directed towards the torch. Light emitted by atoms of metals from samples in plasma was then adapted to quantifiable electrical signals. Standards (Al, Ti, and V 1000 ppm) (Perkin Elmer, Waltham, MA) were used for the generation of linear responses using deionized water and 2% nitric acid (HNO_3). A solution of 2% HNO_3 was used in the calibration as a blank. Calibration concentrations ranged from 0 to 150 ppm for all analyzed elements.

2.3 Surface Characterization

Microscopic analysis of the implant specimens was performed to evaluate the amount of surface damage present. A preliminary visual inspection was used to first identify areas of interest on all specimens, which were then further investigated at higher magnifications. Optical microscopy images were taken using both low and high magnifications (300x to 500x) in high dynamic range mode (HDR) (Keyence VHX-2000). Further surface morphological features, biological deposits, and metallic imperfections (pit-like formations, delamination) from wear were seen on the surface of implants using scanning electron microscopy (SEM) in high vacuum mode (SEM/EDS, JEOL SM-6010LA, Jeol Peabody, MA). SEM images were again taken at higher magnification (1000x). For each of the three large regions of interest on a specimen seen via OM, three specific areas were chosen, yielding a total of nine specific regions per implant. The surface areas of features such as localized pits and delamination on the SEM images from each specific region were quantified and averaged as a percentage using Image J software (ImageJ, National Institutes of Health, Bethesda, MD). The implant specimens were ranked using a point-based system, wherein defects such as pitting, fractures, discoloration, and degree of delamination were assigned values based on the averaged Image J numerical data.

2.4 Composition Analysis

Surface elemental composition and oxidation layer thicknesses of retrieved and control (non-implanted) titanium alloy (Ti6Al4V) and stainless-steel (SS) screws were determined using X-ray Photoelectron Spectroscopy (XPS, PHI 5000 Versa Probe II, Physical Electronics Inc., Chanhassen, MN, USA). Screws were selected as a consistent specimen that was common in all patients. Three different areas were selected from the bone contacting thread area per specimen at random. Measurements were taken at an angle of 45° in relation to the sample surface using a monochromatic Al K source of 1486.6 eV. The pressure in the analysis chamber was kept below 10^{-8} torr, and the survey spectra were obtained using a pass energy

of 187.850 eV and 0.8 eV step size. The high-resolution spectra were acquired using a pass energy of 23.5 eV and step size of 0.2 eV. Both types of scans were acquired with charge neutralization enabled in order to eliminate surface charging caused by large amount of adventitious carbon. The regions scanned each had area dimensions of approximately 200 mm^2. In general, the anodization treatment resulted in varying thicknesses of the oxide layer that can visually be seen in the colored surface [27]. Screws were separated into Ti6Al4V (further separated based on oxide color into blue, green, gold and grey) and SS groups. The depth profile of the passivation layer was determined by sputtering the surface with an argon source (1 kV) until the oxygen peak could no longer be detected or became static with bulk elemental states being detected, and the oxide thickness was estimated on sputtering times for standard titanium oxide samples of known thickness (50 μm). Elemental composition of Ti6Al4V screws was further verified and quantified using energy-dispersive X-ray spectroscopy (EDS) in high vacuum mode (SEM/EDS, JEOL SM-6010LA, Jeol Peabody, MA) using method ASTM E1508. For each element, the weight % of that element is the difference between 100% and the total of all other elements.

2.5 Analysis of Corrosion Behavior

Evaluation of corrosion behavior was analyzed with respect to different fluidic/environmental conditions, implant material, and surface anodization. Electrochemical testing of specimens from retrieved implants and disk specimens (n = 3 after immersion in various electrolyte solutions that were representative of diabetic and non-diabetic environments (Table 2)) was performed using a potentiostat (Interface 1000, Gamry Instruments) and a standard three-electrode electrochemical cell setup per ASTM F2129–15. The working electrode was the specimen being tested, the reference electrode was a saturated calomel electrode (SCE), the counter electrode was a graphite rod, and the electrolyte was PBS kept at 37 °C under naturally aerated conditions. Prior to testing, samples were mounted with an alligator clip, wrapped with electrical tape, and further covered with parafilm to prevent condensation and possible fluid contact with the alligator clip. During testing, the open-circuit potential (OCP) was monitored first for one hour to ensure electrochemical equilibrium was sufficiently achieved. The final value was recorded as the corrosion potential (Ecorr). Linear polarization resistance measurements were then conducted within ±10 mV of Ecorr at a scan rate of 0.1667 mV/s based on ASTM G59–05. Afterward, anodic Tafel plots were obtained for the same specimen by polarizing the sample from Ecorr to 250 mV above Ecorr at a scan rate of 1 mV/s in the anodic direction. The corrosion potential (Ecorr) measured from the Tafel plots was determined to be similar in value (±2 mV) to the value measured after OCP monitoring which ensured that no samples were significantly changed during polarization resistance measurements. Based on the extrapolated corrosion current density (icorr), the corrosion rate (CR) was calculated per ASTM G102–89.

2.6 Statistical Analysis

Two-way ANOVA followed by post hoc Tukey’s test was employed to detect any significant differences between mean values of the measured parameters (a = 0.05). The factors were the (i) type of screws based on bulk material and anodization and (ii) immersion media.

3. Results

3.1 Retrieval Study

3.1.1 Surface Characterization—All Ti6Al4V and SS implants exhibited features that are characteristic of surface damage including discoloration, scratches, potential pit-like features, and delamination that were seen through OM and SEM analysis (Figure 1) with red arrows indicating representative areas of damage observed. Discoloration was seen on all retrieved implants. Visual discoloration of the screws was observed to be mainly at the head and the grooves of the threads. Delamination suggested that the area bore large mechanical stress and was primarily concentrated at the junctions of screws and rods. Aside from mechanical stress, many of the screw heads had large and deep abrasive scratches, possibly created either during implantation or retrieval. Analysis of the SEM images with Image J revealed the presence of pit-like features (shown in dark regions) and discoloration ranging from 1% to 24% of the surface area. Pit-like features were primarily seen at junction regions of specimens that consisted of multiple metallic components (screws with plates, or screws with rods), which is inducive to galvanic corrosion.

3.1.2 Surface Chemical Composition Analysis—Energy-dispersive X-ray spectroscopy (EDS) was used to evaluate differences in the atomic composition of bulk material of randomly selected titanium screws between non-diabetics and diabetics (Table 3). The Ti6Al4V alloy's respective elements (Ti, Al, and V) were observed with the rest of the chemical makeup primarily consisting of C, N, P, Si, and O. Although no significant differences were seen between the non-implanted control, or implants from diabetic and non-diabetic patients, there was a higher standard deviation observed for oxygen and titanium in the implants retrieved from diabetic patients.

3.1.3 Oxide Thickness (XPS)—To correlate the oxide thickness of orthopedic screws based on bulk material and anodization treatment, XPS measurements of Ti6Al4V and SS screws (Figure 2) were compared to controls. In general, XPS analysis revealed thinner oxide layers for all Ti6Al4V (excluding Grey Type II anodized implants) and SS surfaces of implants compared to controls. Also, all explanted Ti6Al4V screws had thicker average oxide layers compared to SS samples. Ti oxide thickness increased in the following order: Yellow<Blue<Green< Control<Grey.

3.1.4 Corrosion Behavior—To evaluate the corrosion behavior between the bulk material and type of anodization treatment of controls and explanted screws, the corrosion rate (Figure 3 A) and polarization values (Figure 3 B) were quantified and compared. Screws were separated into Ti6Al4V and SS groups. Ti6Al4V groups had been originally manufactured to have blue, green, gold and grey II (indicative of "Type II anodization") surfaces. Corrosion rates for Ti6Al4V retrieval specimens were lower than the control group and correspondingly had higher polarization resistance values than control group. Stainless steel retrieval specimens had higher corrosion rates compared to the control group samples, and correspondingly had lower polarization resistance values. Despite the lack of significant difference being observed, Ti specimens had ~2–10 times lower average corrosion rate

values than control Ti6Al4V control while SS specimens had ~10 times higher average corrosion rate values than non-implanted SS control ($p > 0.05$).

3.2 *In vitro* Analysis of Particle Release under Simulated Diabetic Conditions

3.2.1 Particle Release—To assess the influence of surrounding fluidic environment on the metal surface, the concentration of Ti and Al particles leached into three types of immersion fluids (DMEM, artificial saliva, and PBS) after 28 days at 37 °C is shown in Figure 4. Titanium alloy (Ti6Al4V) disks were immersed in various fluids (DMEM (Figure 4 A–B), artificial saliva (Figure 4 C–D), and PBS (Figure 4 E–F)) that contained solutes (glucose, urea, and beta hydroxybutyrate (B-OH)) representing an implant surface in simulated diabetic and non-diabetic conditions. Titanium ions were detected in higher concentrations post-immersion in DMEM and PBS for all treatment groups except DMEM HU versus non-immersed DMEM or PBS control groups but was not significantly different ($p > 0.05$). In artificial saliva, Ti ion release was also higher on average post-immersion as compared to control groups and was statistically increased for LG ($p = 0.0327$) and LB ($p = 0.0214$) treatments. Similarly, aluminum ions were found at elevated levels in all treatments post-immersion relative control but were only significantly different in artificial saliva for the non-treated blank and diabetic concentrations of glucose HG ($p < 0.0001$), urea HU ($p < 0.0001$), and beta-hydroxybutyrate (HB) ($p = 0.0001$). Vanadium ion concentrations were below the limit of detection for all immersion groups.

To evaluate the influence of the metal to the surrounding fluidic environment, the pH levels were recorded pre- and post-immersion for the three types of immersion fluids (DMEM, artificial saliva, and PBS) after 28 days at 37 °C (Figure 5). Solutions made with DMEM showed slight increases of pH post-immersion but were not significantly different ($p > 0.05$). Artificial saliva solutions were generally more acidic than their DMEM/PBS counterparts. Artificial saliva solutions primarily showed increases in the pH values post-immersion, but the only treatment that was significantly different was diabetic concentration of urea (HU). The pH of the non-treated saliva post-immersion also significantly decreased versus pre-immersion ($p = 0.0253$). PBS groups showed minor decreases in pH but did not result in significant pH changes post-immersion compared to pre-immersed solutions ($p > 0.05$).

3.2.2 Corrosion Behavior—To analyze the *in vitro* influence of simulated diabetic conditions to metallic surfaces, the corrosion characteristics (corrosion rates (Figure 6A) and polarization resistance (Figure 6B)) of Ti6Al4V disks were evaluated post-immersion in three types of immersion fluids (DMEM, artificial saliva, and PBS) after 28 days at 37 °C. In general, all immersed groups had higher corrosion rates than non-immersed groups, but the average corrosion rate and polarization resistance values of Ti6Al4V immersed in DMEM, artificial saliva and PBS were not observed to be significantly different as compared to controls ($p > 0.05$). The highest corrosion rate was seen in artificial saliva with low urea concentration when compared to the citric acid positive control and immersion control but was not significantly different from other treatments ($p > 0.05$). DMEM with beta-hydroxybutyrate showed higher corrosion rates correspondent to higher concentrations (HB compared to LB). The reverse trends are observed for polarization resistance values.

4. Discussion

It is critical to determine the diabetic specific mechanisms underlying poor osseointegration between metallic implants and bone tissue. The overall goal of this study was to investigate orthopedic implant surface characteristics that could elucidate mechanisms of implant material degradation. The research question of why implants fail at a higher rate for diabetic patients was addressed by microscopic and spectroscopic techniques. The results demonstrated that all retrieved implants (from non-diabetic and diabetic patients) suffered a wide range of surface damage including pitting attack, discoloration, scratches, and delamination (Figure 1). Although implants received from diabetic patients had higher standard deviations in the amount of oxygen and titanium present at the surface (Table 3), the results demonstrated no significant differences in the surface chemical composition of retrievals between non-diabetic or diabetic groups. There are notable changes in compositions between biological fluids of diabetic patients compared to non-diabetic patients that can potentially be key causative factors in the degradation of the surface layer of metallic implants. Topography of the implant surface have also been found to clinically affect osseointegration by changing the mechanical properties of implants and influencing cell responses. Physical damage to implant surfaces and subsequently oxide layer decreases both osteoblast proliferation and osseointegration integrity.

It is likely that changes to implanted materials begin to occur immediately after implantation due to the varying biological environment where changes in fluids, proteins, mechanical, and chemical loads can occur simultaneously. Discoloration occurs through electrochemical interactions with adherent proteins and surrounding fluids that create acidic peri-implant conditions and triggers oxidation of the surface [5]. *In vivo*, galvanic corrosion is possible if two different metals are present and electrochemically interact through fluids (synovial fluid, blood, etc.). It is presumed that galvanic corrosion occurred primarily where stainless steel and Ti6Al4V materials were used conjointly, leading to a depassivation of a localized area that became anodic. Pitting consistent with those seen through SEM analysis in the literature [28] were observed, indicating that local inclusions or grain boundaries at the surface were subject to anodic attack (Figure 1). Delamination suggests a force was applied to the implant surface, which could induce microcracking that results in buckling. These forces may have been applied by the surgeon during either implantation or extraction, from external forces applied to the implant site during the healing process, tribocorrosion, micromotion, or an aggregate of these factors [5].

The presence of surface damage-related products or electrochemical redox interactions at the surface of unoxidized metal can increase the rate at which metal ions are leeched into the local biological environment [5]. Substantial necrosis has been seen in periprosthetic tissues due to metal ion release, that lead to implant loosening [29]. Metal ion release is a concern because it can lead to adverse tissue responses, specifically for patients that already have chronic forms of inflammation. Through ICP-OES analysis (Figure 4), higher amounts of aluminum ions from Ti6Al4V under simulated non-diabetic and diabetic conditions were observed to be released into the immersion solutions while relatively low amounts of titanium particles were released. The release of aluminum ions was significantly higher for diabetic conditions in artificial saliva as compared to non-diabetic artificial saliva conditions,

which is consistent with implant failure rates seen in the oral environment of diabetic and non-diabetic patients [30].

This may be due in part to the lower scratch hardness of Al compared to Ti, causing the material to leach out from the bulk material at a faster rate [31]. Aluminum has been shown to interact with calcium and has a strong affinity for phosphate [31]. Aluminum ions can accumulate at the bone surface, where it preferentially binds to the unmineralized type I collagen. The binding impairs calcification and may also contribute to the secondary suppression of parathyroid hormone secretion (which regulates serum calcium), which can result in osteomalacia and increased pain [32]. Vanadium ions were not detected through ICP-OES, which may be due to vanadium being found in significantly lower amounts within the bulk material, thus potentially releasing ions below the detection level. Studies have shown increased vanadium concentrations surrounding implants that have surface damage from wear [11], which did not occur during simulated immersion procedures. Although titanium ions were “detected” pre-immersion in DMEM samples, there is a high possibility of baseline noise or spectral overlap (Ti emission spectra: 323 nm and 335 nm) from calcium (emission: 317 nm and 315 nm) or sodium (emission: 330 nm) found as ingredients in DMEM as calcium chloride or sodium chloride/ sodium, respectively. Post-immersion ion release analysis showed increased concentrations of ions, making spectral overlap negligible.

The influence of the metal ion release to the surrounding fluidic environment was further shown through pH levels of immersion fluids that generally became slightly more basic post-immersion for the three types of immersion fluids (Figure 5). The anionic OH^- found in immersion fluids interacts with cationic Al^+ and Ti^+, making the surrounding solutions more basic. Although the pH pre- and post-immersion was not significantly different, we did observe slightly lower alkalinity in the PBS immersion solution. According to the medium’s supplier, the formulation for PBS contains potassium phosphate monobasic (KH_2PO_4), sodium chloride (NaCl), and sodium phosphate dibasic (Na_2HPO_4-$7H_2O$). In aqueous solution, these components will dissociate. Remaining anions are PO_4^{-3}, HPO_4^{-2}, and $H_2PO_4^{-1}$ and can potentially interact with Al^+ and Ti^+ cations. Aluminum has been shown to have a very strong affinity for phosphate [31]. K and Na are spectator ions that dissociate in aqueous solutions, which become ineffective conjugate bases, thus lowering the surrounding alkalinity.

The properties of the titanium oxide layer can influence the biocompatibility of implants. It’s thickness results in unique surface colors that are often used by surgeons to quickly differentiate implant components [27, 33]. When oxide layers are thinner, the potential of exposed bulk material to release metal ions into the surrounding tissues increases, which may induce destructive immune response mechanisms [5]. While anodization modifications for orthopedic implants are currently being studied, the parameters have been found to be extremely sensitive and minute changes may result in altered properties of the oxide films. This makes establishing an industry wide standard for optimal osseointegration while preventing corrosion difficult [27]. Anodization creates a crystal lattice oxide layer that refracts light differently in response to thickness, creating different colors (known as Type 3 anodization). Through XPS analysis (Figure 2), each titanium alloy colored group of implants exhibited different oxide thicknesses in an order that was consistent with the

literature [27] but had an overall decrease of at least 25 nm for implanted specimens (Blue Ti- 26 nm, Green Ti- 37 nm Gold Ti- 23 nm). A different type of anodization is Type 2 anodization that penetrates the surface, forming a much thicker passivation layer resulting in the unique matte grey color. Type 2 anodization increases wear-resistance between sliding titanium surfaces. With regards to corrosion, the oxide film can deteriorate in acidic environments, exposing an unprotected metal that is oxidized to the violet colored soluble trivalent ion (Ti^{3+}). This trivalent ion can further oxidize into a pale yellow Ti^{4+} ion in the abundant presence of oxidizing species[34, 35]. The relative number of oxygen atoms in each specimen is assumed to be present as metal oxide, which was quantified using EDS. EDS data (Table 3) demonstrated that the average percent of oxygen was found in greater standard deviations observed for retrieved titanium screws from diabetic patients, as opposed to non-diabetic patients or control screws. A similar comparison could not be made for stainless steel screws due to the lack of these specimens for the diabetic group. For stainless steel, Cr in its oxide form (Cr_2O_3) is the primary oxide component and can be damaged easily by the fluidic environment [36]. Stainless steel implants usually have a much thinner oxide layer (2–4 nm) prior to implantation [36] but XPS analysis in the present study revealed thicker passivation layers in both implanted (8–12 nm) and control specimens (33–37 nm), which can be attributed to potential surface coatings. Furthermore, the oxide thickness based on XPS of the retrievals was thinner on average than controls. Electrochemical testing (Figure 3) showed that these specimens actually had lower corrosion rates than the controls. This behavior indicates that the longer implantation and thus exposure of the surface to biological fluids allowed the oxide layer to become more electrochemically stable *in vivo*, which correlates to the lower corrosion rates in implanted specimens compared to controls [37]. The only exception was the Grey Ti alloy screws, which underwent Type II anodization treatment that imparts thicker passivation layer [27]. Ion leeching from damaged oxide layers can be further exacerbated by microparticles produced during implant surgery [14]. Tissues immediate to compromised stainless steel implants may be affected by hydrated ferric oxide byproducts of iron that can lead to hemosiderosis if not treated quickly [38].

Corrosion occurs through redox reactions that are heavily influenced by the contents of the surrounding liquid medium. The corrosion properties of metals tested were expected to be unique to each of the solution-solute combinations (DMEM, artificial saliva, and PBS, each with high and low concentrations of glucose, urea, beta-hydroxybutyrate). For the metal disks, the oxide that formed pre-immersion generally remained intact post-immersion due to the simpler testing environment (known solutes/solution as opposed to proteins and inflammation experienced by the implanted devices *in vivo*) [38]. During immersion, a denser protective layer formed based on the fluid properties, which was demonstrated through electrochemical testing results after immersion in simulated diabetic environments (Figure 6). Similarly, the corrosion properties of titanium screws and stainless-steel screws (Figure 3) were found to not show any significant differences between each group, indicating that SS and Ti alloy implants are expected to respond similarly under *in vivo* conditions. Despite surface damages seen on implant retrievals through SEM, the overall oxide layer was electrochemically more stable for implanted components compared to control implants. Although titanium and stainless steel spontaneously form an oxide layer,

imperfections from applied mechanical forces or fluid interactions could lead to oxide thinning and exposure of the bulk material to bodily fluids.

There were no distinctive signs of surface damage that were correlated directly with diabetes, which may suggest that the orthopedic implants evaluated in this study underwent similar levels of surface degradation regardless of the acidic or hyperglycemic environment that is characteristically seen in diabetics. However, higher failure rates seen in diabetic patients undergoing orthopedic surgery can instead be attributed to their inflammatory response or impaired healing mechanisms [2]. Due to hyperglycemia, diabetics have increased advanced glycation end products that inhibit the formation of bone forming cells at early healing stages [39]. Out of 39 implants that were received, 35.9% were from diabetic patients, with the highest percentage of those implants coming from the ankle, foot, and legs (Table 1).

Retrieval studies have been challenging due to difficulties in assembling larger implant pools for analysis [9]. Some of the limitations in this study were that not all implants were from the same area of the body (tibia, femur, wrist, foot, etc.), or were made from the same material (titanium alloy vs. stainless steel alloy). It is challenging to accurately predict how surrounding tissues will interact with a surface, and in turn how an implant surface will respond to an *in vivo* environment subject to the large variability of inflammatory responses. Although the immersion solutions used in the *in vitro* experiments attempted to simulate diabetic and non-diabetic conditions, the lack of applied mechanical stresses, adherent proteins, and macrophages that would have better simulated the ion release seen *in vivo* can have major effects on the amount of corrosion observed. The synergy of cyclic loads and acidic environments would promote a more physiologically relevant scenario that could have impacted the surface differently. In order to better determine how implants can have more stable surface interfaces, a relationship between the amount of decay of the implant surface and the surrounding microenvironment needs to be further established. Future studies will explore larger pools of retrieved specimens to investigate surface damages seen due to variations in implantation/retrieval techniques and correlate patient lifestyles and clinical factors that may influence the success of the implant.

5. Conclusion:

All retrieved implants suffered a wide range of surface damage seen through pitting attack, discoloration, scratches, and delamination in addition to thinner oxide layers. The *in vitro* analysis showed that there was higher aluminum ion release from Ti alloy in diabetic conditions in saliva that corresponded to more acidic environments. Regardless of the environment from where the implants were obtained or the testing conditions, the corrosion properties were similar for diabetic and non-diabetic groups. This finding may indicate that orthopedic failures can be attributed to other biological factors that impair osseointegration at early stage events in the healing. These results are important because they will be subsequently correlated with specific factors from the clinical profiles to help elucidate associations between the biological significance of diabetes to implant failure. As the population affected by diabetes increases and the field of orthopedics evolves, it becomes

even more critical to establish correlations that could potentially yield innovations that lead to increased rates of both short- and long-term orthopedic implant retention.

Acknowledgments:

The authors would like to acknowledge the support from the National Institute of Diabetes and Digestive and Kidney Diseases (NIDDK/NIH) F31 fellowship number DK121483-01. This project is also supported by the University of Texas at Dallas (UTD) Office of Research through a seed grant, Collaborative Biomedical Research Award (CoBRA). We thank Danyal Siddiqui for his expertise and manuscript edits.

Funding: This research was supported by the NIH Ruth L. Kirschstein National Research Service Award (NRSA) Individual Predoctoral Fellowship to Promote Diversity in Health-Related Research (F31DK121483-01) Award and the Eugene McDermott Fellowship.

References

1. Ciampolini J, Hubble MJW (2005) Early failure of total hip replacements implanted at distant hospitals to reduce waiting lists. Ann R Coll Surg Engl 87:31. 10.1308/1478708051450 [PubMed: 15720905]
2. Kumar V, Patel BY, Robinson AH (2019) Diabetes and orthopaedic surgery: a review. Orthop Trauma 33:212–216. 10.1016/J.MPORTH.2019.05.002
3. Statistics About Diabetes | ADA. https://www.diabetes.org/resources/statistics/statistics-about-diabetes. Accessed 12 May 2020
4. Wukich DK (2015) Diabetes and its negative impact on outcomes in orthopaedic surgery. World J. Orthop. 6:331–339 [PubMed: 25893176]
5. Eliaz N (2019) Corrosion of Metallic Biomaterials: A Review. Materials (Basel) 12:407. 10.3390/ma12030407
6. Trindade R, Albrektsson T, Tengvall P, Wennerberg A (2016) Foreign Body Reaction to Biomaterials: On Mechanisms for Buildup and Breakdown of Osseointegration. Clin Implant Dent Relat Res 18:192–203. 10.1111/cid.12274 [PubMed: 25257971]
7. Cadosch D, Al-Mushaiqri MS, Gautschi OP, et al. (2010) Biocorrosion and uptake of titanium by human osteoclasts. J Biomed Mater Res Part A 95A:1004–1010. 10.1002/jbm.a.32914
8. Huber M, Reinisch G, Trettenhahn G, et al. (2009) Presence of corrosion products and hypersensitivity-associated reactions in periprosthetic tissue after aseptic loosening of total hip replacements with metal bearing surfaces. Acta Biomater 5:172–180. 10.1016/J.ACTBIO.2008.07.032 [PubMed: 18725188]
9. Anderson JM, Brown SA, Merrit K (2013) Implant Retrieval and Evaluation. Biomater Sci 1368–1383. 10.1016/B978-0-08-087780-8.00128-5
10. Zink TM, McGrory BJ (2020) Mechanically Assisted Crevice Corrosion in a Metal-on-Polyethylene Total Hip Presenting With Lower Extremity Vascular Compromise. Arthroplast today 6:445–450. 10.1016/j.artd.2020.04.015 [PubMed: 32637514]
11. Santos CT dos, Barbosa C, Monteiro M de J, et al. (2015) Fretting corrosion tests on orthopedic plates and screws made of ASTM F138 stainless steel. Res Biomed Eng 31:169–175. 10.1590/2446-4740.0710
12. Pincus D, Veljkovic A, Zochowski T, et al. (2017) Rate of and Risk Factors for Intermediate-Term Reoperation After Ankle Fracture Fixation. J Orthop Trauma 31:e315–e320. 10.1097/BOT.0000000000000920 [PubMed: 28614147]
13. Giacco F, Brownlee M (2010) Oxidative stress and diabetic complications. Circ Res 107:1058–70. 10.1161/CIRCRESAHA.110.223545 [PubMed: 21030723]
14. Finnerty CC, Mabvuure NT, Ali A, et al. (2013) The surgically induced stress response. JPEN J Parenter Enteral Nutr 37:21S–9S. 10.1177/0148607113496117 [PubMed: 24009246]
15. Frydrych LM, Fattahi F, He K, et al. (2017) Diabetes and Sepsis: Risk, Recurrence, and Ruination. Front Endocrinol (Lausanne) 8:271. 10.3389/fendo.2017.00271 [PubMed: 29163354]

16. Jämsen E, Nevalainen P, Eskelinen A, et al. Obesity, Diabetes, and Preoperative Hyperglycemia as Predictors of Periprosthetic Joint Infection A Single-Center Analysis of 7181 Primary Hip and Knee Replacements for Osteoarthritis. 10.2106/JBJS.J.01935
17. Boström KI, Jumabay M, Matveyenko A, et al. (2011) Activation of vascular bone morphogenetic protein signaling in diabetes mellitus. Circ Res 108:446–57. 10.1161/CIRCRESAHA.110.236596 [PubMed: 21193740]
18. Feng Y-F, Wang L, Zhang Y, et al. (2013) Effect of reactive oxygen species overproduction on osteogenesis of porous titanium implant in the present of diabetes mellitus. Biomaterials 34:2234–43. 10.1016/j.biomaterials.2012.12.023 [PubMed: 23294547]
19. Tamam E, Turkyilmaz I (2014) Effects of pH and Elevated Glucose Levels on the Electrochemical Behavior of Dental Implants. J Oral Implantol 40:153–159. 10.1563/AAID-JOI-D-11-00083 [PubMed: 24779948]
20. Lin T-H, Hu H-T, Wang H-C, et al. (2017) Evaluation of osseous integration of titanium orthopedic screws with novel SLA treatment in porcine model. PLoS One 12:. 10.1371/JOURNAL.PONE.0188364
21. Mabilleau G, Bourdon S, Joly-Guillou ML, et al. (2006) Influence of fluoride, hydrogen peroxide and lactic acid on the corrosion resistance of commercially pure titanium. Acta Biomater 2:121–129. 10.1016/J.ACTBIO.2005.09.004 [PubMed: 16701867]
22. Wei W, Liu Q, Tan Y, et al. (2009) Oxidative Stress, Diabetes, and Diabetic Complications. Hemoglobin 33:370–377. 10.3109/03630260903212175 [PubMed: 19821780]
23. Kang C-W, Fang F-Z (2018) State of the art of bioimplants manufacturing: part I. Adv Manuf 6:20–40. 10.1007/s40436-017-0207-4
24. Hill NR, Oliver NS, Choudhary P, et al. (2011) Normal reference range for mean tissue glucose and glycemic variability derived from continuous glucose monitoring for subjects without diabetes in different ethnic groups. Diabetes Technol Ther 13:921–8. 10.1089/dia.2010.0247 [PubMed: 21714681]
25. Higgins C (2016) Urea and the clinical value of measuring blood urea concentration
26. Lima-Aragão MVV, Oliveira-Junior J de J de, Maciel MCG, et al. (2016) Salivary profile in diabetic patients: biochemical and immunological evaluation. BMC Res Notes 9:103. 10.1186/S13104-016-1881-1 [PubMed: 26879274]
27. İzmir M, Ercan B (2019) Anodization of titanium alloys for orthopedic applications. Front Chem Sci Eng 13:28–45. 10.1007/s11705-018-1759-y
28. Astarita A, Curioni M, Squillace A, et al. (2015) Corrosion behaviour of stainless steel-titanium alloy linear friction welded joints: Galvanic coupling. Mater Corros 66:111–117. 10.1002/maco.201307476
29. Mahendra G, Pandit H, Kliskey K, et al. (2009) Necrotic and inflammatory changes in metal-on-metal resurfacing hip arthroplasties: Relation to implant failure and pseudotumor formation. Acta Orthop 80:653. 10.3109/17453670903473016 [PubMed: 19995315]
30. Naujokat H, Kunzendorf B, Wiltfang J (2016) Dental implants and diabetes mellitus-a systematic review. Int J Implant Dent 2:5. 10.1186/s40729-016-0038-2 [PubMed: 27747697]
31. Manam NS, Harun WSW, Shri DNA, et al. (2017) Study of corrosion in biocompatible metals for implants: A review. J Alloys Compd 701:698–715. 10.1016/J.JALLCOM.2017.01.196
32. Klein GL (2019) Aluminum toxicity to bone: A multisystem effect? Osteoporos Sarcopenia 5:2–5. 10.1016/j.afos.2019.01.001 [PubMed: 31008371]
33. Napoli G, Zitelli C, Corapi D, di Schino A (2018) Titanium Alloys Anodic Oxidation: Effect of Experimental Parameters on Surface Colouring. Mater Sci Forum 941:730–734. 10.4028/www.scientific.net/MSF.941.730
34. Bhola R, Bhola SM, Mishra B, Olson DL (2010) Corrosion in Titanium Dental Implants/Prostheses - A Review. Trends Biomater Artif Organs 25:34–46
35. Rodrigues DC, Valderrama P, Wilson TG, et al. (2013) Titanium Corrosion Mechanisms in the Oral Environment: A Retrieval Study. Mater (Basel, Switzerland) 6:5258–5274. 10.3390/ma6115258
36. Mandrino D, Godec M, Torkar M, Jenko M (2008) Study of oxide protective layers on stainless steel by AES, EDS and XPS. Surf Interface Anal 40:285–289. 10.1002/sia.2718

37. Gugelmin BS, Santos LS, Ponte H de A, et al. (2015) Electrochemical Stability and Bioactivity Evaluation of Ti6Al4V Surface Coated with Thin Oxide by EIS for Biomedical Applications. Mater Res 18:602–607. 10.1590/1516-1439.201514

38. Corradetti B, Impact T (2017) The Immune Response to Implanted Materials and Devices

39. Biguetti CC, Cavalla F, Silveira EV, et al. (2019) HGMB1 and RAGE as Essential Components of Ti Osseointegration Process in Mice. Front Immunol 10:. 10.3389/fimmu.2019.00709

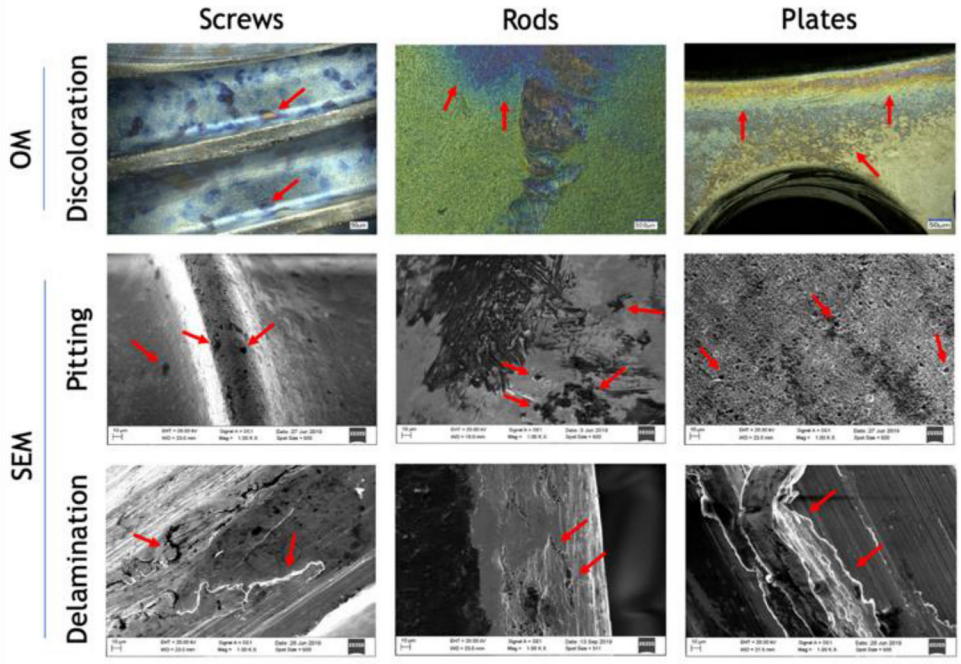

Fig. 1.

Surface characterization of retrieved orthopedic implants demonstrating damages (red arrows) shown through optical microscopy at 300x (top row) and scanning electron microscopy at 1000x (middle and bottom rows) of representative Ti6Al4V and SS screws, rods and plates

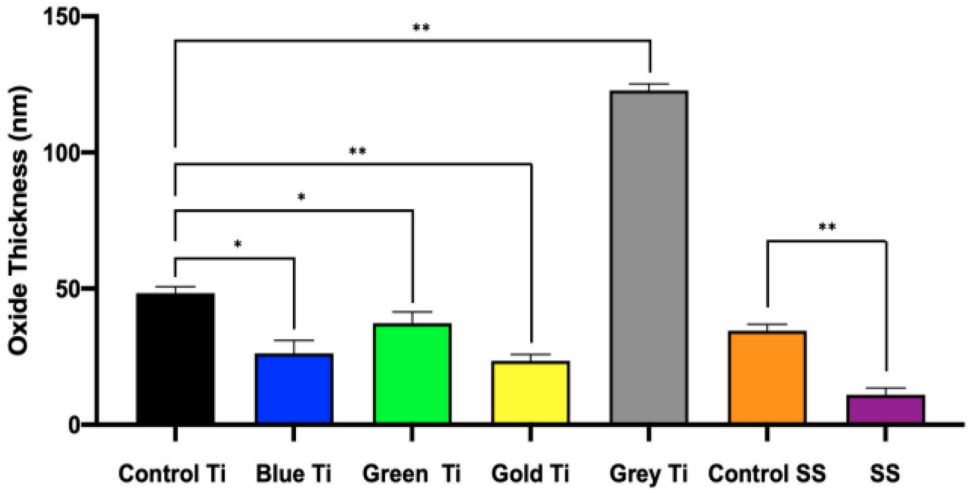

Fig. 2.

X-ray Photon Spectroscopy (XPS) analysis demonstrating oxide layer thickness of orthopedic screws based on anodization color. Data was analyzed at n=3 per sample group. Single asterisk denotes statistical significance ($P < .0097$), double asterisk denotes ($P < .0001$)

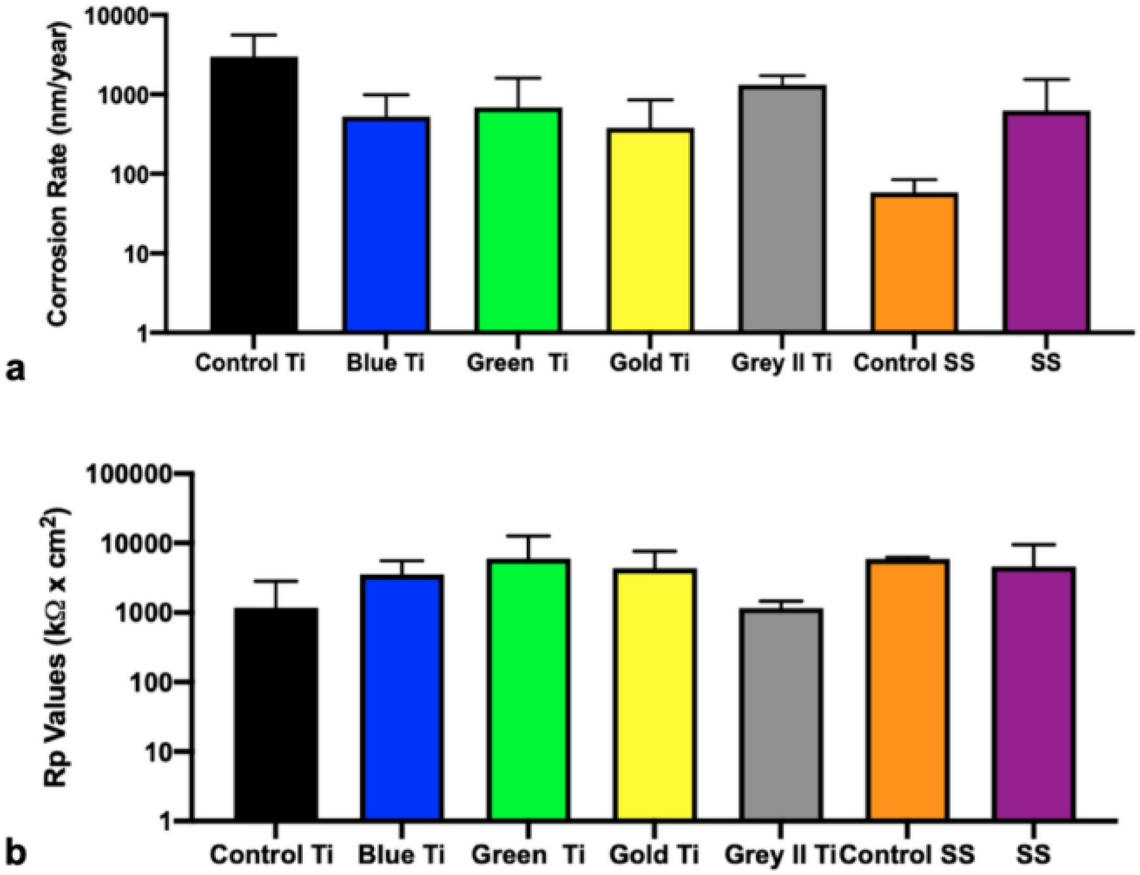

Fig. 3.

Electrochemical (a) corrosion rates and (b) polarization resistance (Rp) values of retrieved implants (screws) separated by material anodization color (n = 3)

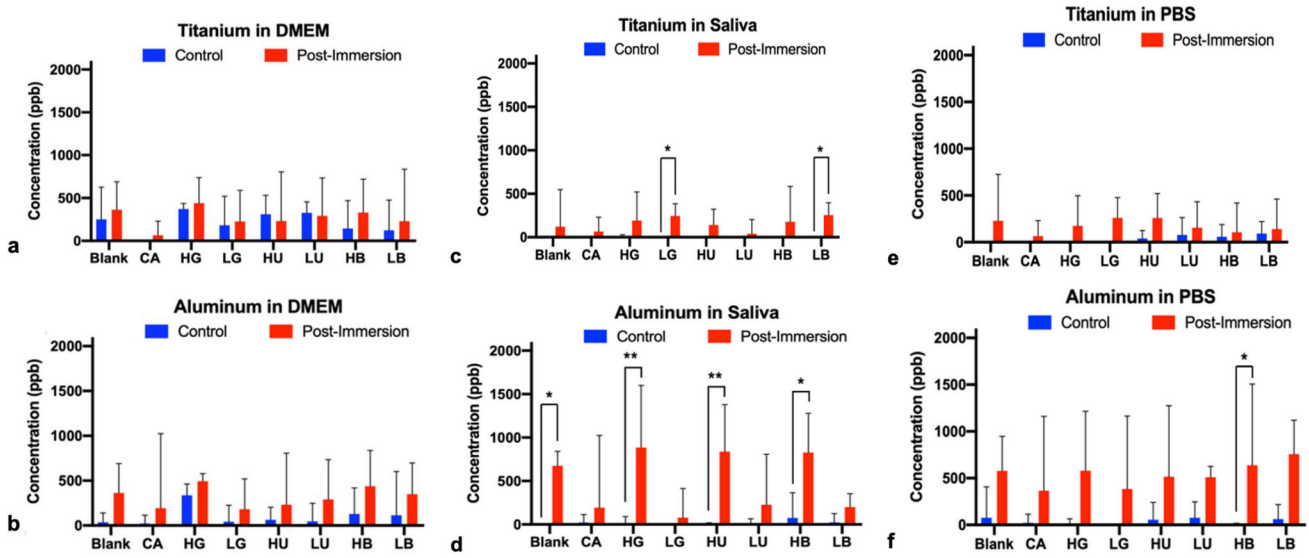

Fig. 4.

a-b Concentration of (a) Ti and (b) Al particles after immersion of Ti6Al4V disks in simulated diabetic (high solute concentration) or non-diabetic (low solute concentrations) for 28 days at 37 °C in various media (DMEM) using ICP-OES. Treatments were citric acid (CA) positive control, glucose in high (HG) and low (LG) concentrations, urea in high (HU) and low (LU) concentrations, beta-hydroxybutyrate in high (HB) and low (LB) concentrations, and the untreated blank control. Single asterisk denotes statistical significance ($P < .0097$), double asterisk denotes ($P < .0001$)

Fig. 4 c-d Concentration of (c) Ti and (d) Al particles after immersion of Ti6Al4V disks in simulated diabetic (high solute concentration) or non-diabetic (low solute concentrations) for 28 days at 37 °C in various media (artificial saliva) using ICP-OES. Treatments were citric acid (CA) positive control, glucose in high (HG) and low (LG) concentrations, urea in high (HU) and low (LU) concentrations, beta-hydroxybutyrate in high (HB) and low (LB) concentrations, and the untreated blank control. Single asterisk denotes statistical significance ($P < .0097$), double asterisk denotes ($P < .0001$)

Fig. 4 e-f Concentration of (e) Ti and (f) Al particles after immersion of Ti6Al4V disks in simulated diabetic (high solute concentration) or non-diabetic (low solute concentrations) for 28 days at 37 °C in various media (PBS) using ICP-OES. Treatments were citric acid (CA) positive control, glucose in high (HG) and low (LG) concentrations, urea in high (HU) and low (LU) concentrations, beta-hydroxybutyrate in high (HB) and low (LB) concentrations, and the untreated blank control. Single asterisk denotes statistical significance ($P < .0097$), double asterisk denotes ($P < .0001$)

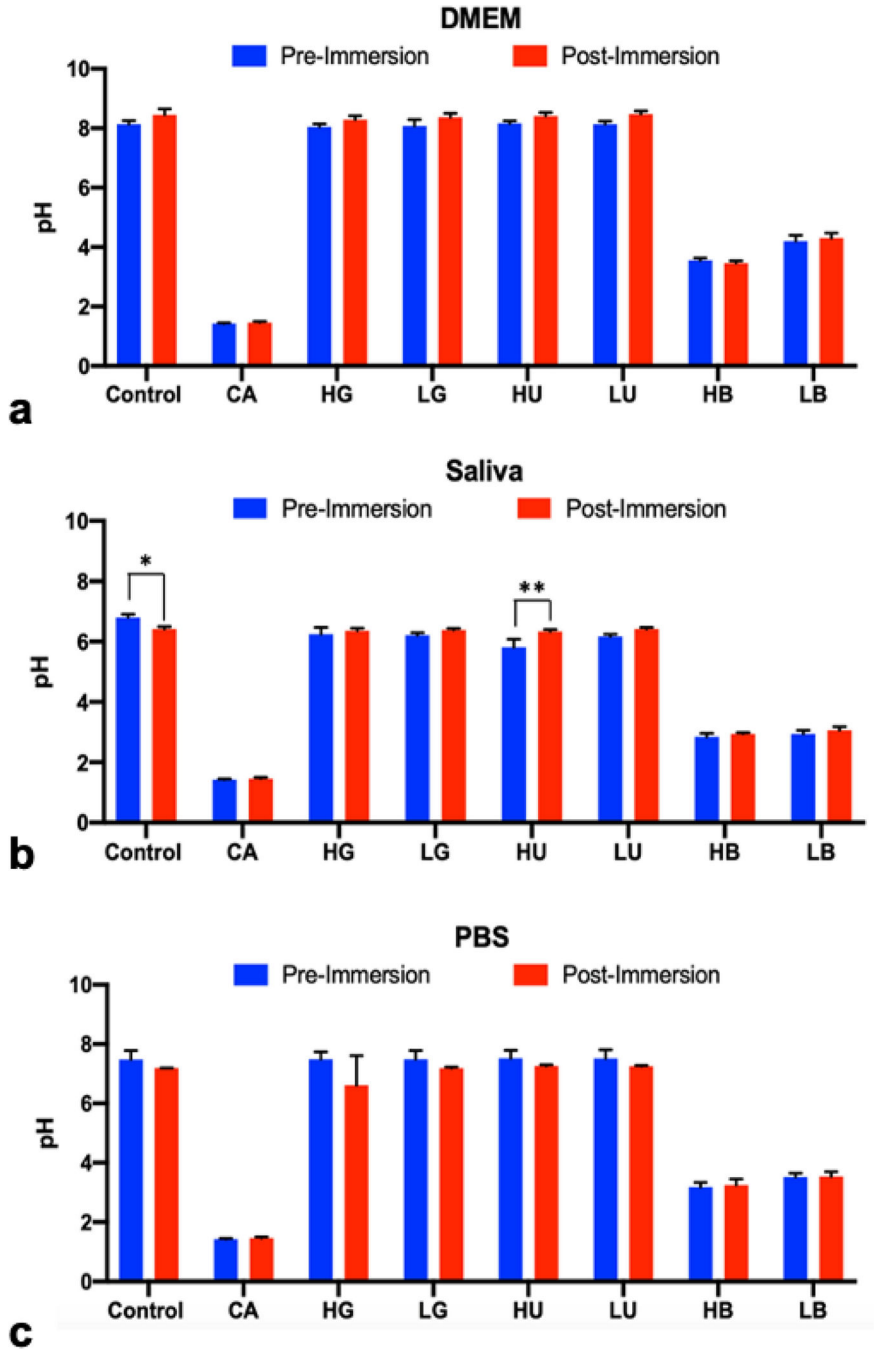

Fig. 5.

pH values of immersion fluids (DMEM (a), artificial saliva (b), and PBS (c)) pre- and post-immersion of Ti6Al4V disks in simulated diabetic (high solute concentration) or non-diabetic (low solute concentrations) for 28 days at 37 °C. Treatments were citric acid (CA) positive control, glucose in high (HG) and low (LG) concentrations, urea in high (HU) and low (LU) concentrations, beta-hydroxybutyrate in high (HB) and low (LB) concentrations, and the untreated blank control. Single asterisk denotes statistical significance ($P < .0097$), double asterisk denotes ($P < .0001$)

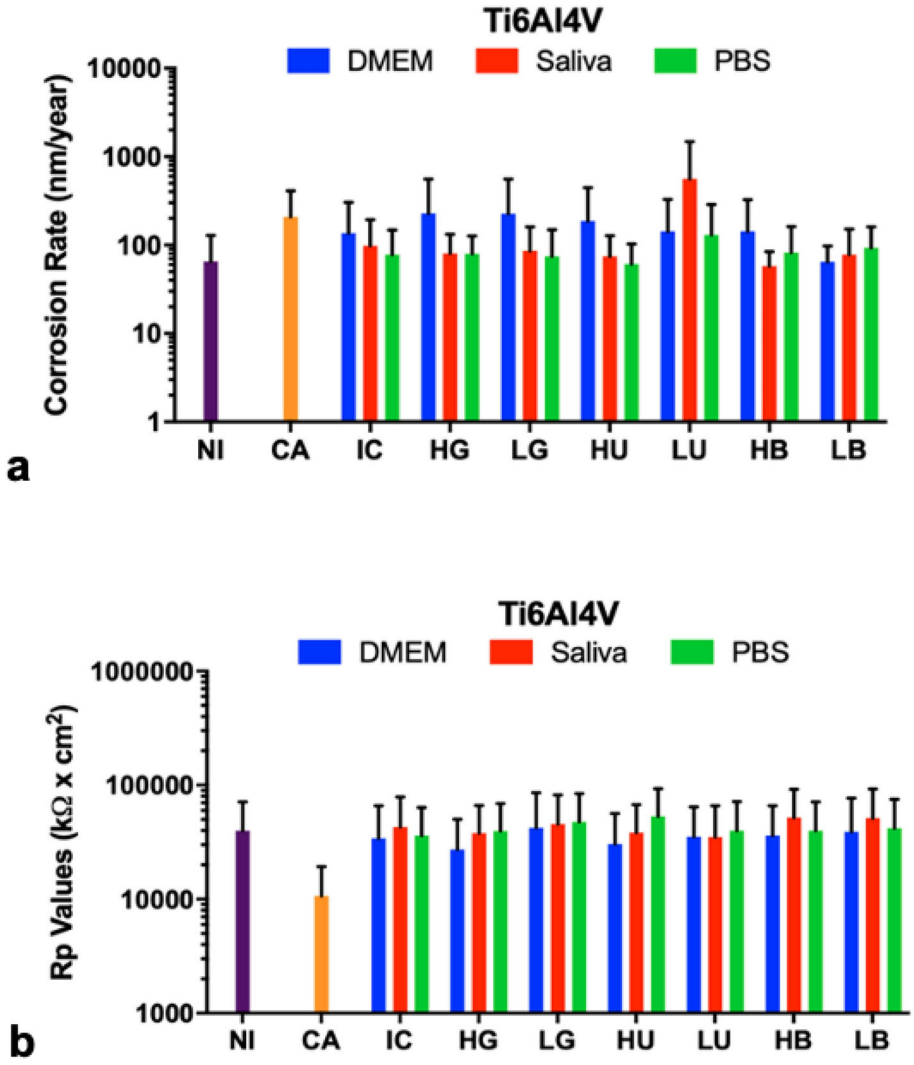

Fig. 6.

Electrochemical corrosion rates (a) and polarization resistance (Rp) values (b) of polished Ti6Al4V disks at n=3 immersed for 28 days at 37 °C. Treatments were citric acid (CA) positive control, glucose in high (HG) and low (LG) concentrations, urea in high (HU) and low (LU) concentrations, beta-hydroxybutyrate in high (HB) and low (LB) concentrations, and the untreated blank control

Table 1.

Summary of specimens evaluated in this study showing number of implants obtained from each location, type of implant, bulk material, and whether they were obtained from diabetic patients.

Location	Type of Implant	Material	Number of Implants	Implants from Diabetics
Ankle	Plate and Screws	SS	7	3
		Ti6Al4V	4	1
		SS and Ti6Al4V	2	1
Foot	Screw	SS	2	1
Leg	Rod/Plates and Screws	Ti6Al4V	8	4
	Plates and Screws	SS	3	1
Femur		Ti6Al4V	3	1
		SS	2	0
	Rods and Screws	SS and Ti6Al4V	1	1
Elbow	Plates and Screws	SS	3	0
Arm/Wrist	Plates and Screws	SS	3	0
	Rod and Screws	Ti6Al4V	1	1

Table 2.

Concentrations of solutes used in biological medias. Each noted solvent was added in concentrations corresponding to diabetic patients and non-diabetic patients identified as “normal.” All concentrations reported in this table are in mg/dL of solution.

	Control	Normal Glucose	Diabetic Glucose	Normal Urea	Diabetic Urea	Normal Beta-OH	Diabetic Beta-OH
DMEM	0	72	200	7	38	40	60
Artificial Saliva	0	3	11	17	27	26	52
PBS	0	72	200	17	38	40	60

Table 3.

EDS table depicting the average weight % of each elemental composition on the surface of titanium screws for diabetics and non-diabetics.

	Control		Diabetic		Non-Diabetic	
	Average	**Standard Deviation**	**Average**	**Standard Deviation**	**Average**	**Standard Deviation**
C	1.010	0.413	1.316	0.801	1.090	0.533
N	2.272	1.472	2.265	1.462	2.282	1.574
O	10.010	3.856	9.584	9.881	10.120	6.882
Na	0.318	0.214	0.407	0.457	0.323	0.312
Al	5.871	1.138	5.915	1.019	5.038	1.513
Si	0.849	0.952	0.590	0.958	1.105	1.855
P	0.237	0.112	0.337	0.283	0.232	0.131
Ca	0.188	0.117	0.272	0.276	0.198	0.127
Ti	76.848	4.545	75.735	10.216	76.151	5.346
V	2.359	0.379	1.768	1.229	2.455	0.269
Fe	0.337	0.075	0.447	0.184	0.312	0.063